

SOURCE PARAMETER MAP — A NEW AID TO AEROMAGNETIC DATA INTERPRETATION*†

S. JAIN**, W. SCHUUR*** and C. E. CURTIS***

ABSTRACT

A filtering technique based on reduction to the pole and residual methods has been developed to assist in the interpretation of total magnetic field data. The results of the technique are presented in the form of a filtered map termed the SOURCE PARAMETER Map or SOPAM. This map shows the outlines of source bodies and the magnetic susceptibility contrast between these bodies and the surrounding material. Empirical depth estimates are also available from the positions of plotted maxima and minima.

As demonstrated by several examples using model data, the SOPAM technique has application in both petroleum and mining surveys as a rapid interpretation tool.

INTRODUCTION

The data collected in an aeromagnetic survey is normally compiled in the form of contour maps which present the total magnetic field due to all sources of anomalies occurring at various levels of depth. The interpretation of the geological events causing the observed magnetic responses involves the recognition of individual causative bodies, and their quantitative description in terms of depth, size, and magnetic susceptibility.

All such quantitative procedures involve the use of model sources, and differ according to the type of model most closely ap-

proximating the source of the anomaly under consideration.

The importance of block-type sources in aeromagnetic interpretation has long been recognized by virtue of the applicability of such sources to a variety of commonly-occurring geological situations. Therefore, of the various models commonly utilized for quantitative interpretation, the infinitely thick, vertically-sided prismatic block has received considerable attention.

This paper discusses a filter to be applied to the final, total field maps which may considerably simplify the process of interpretation. Employing the widely-applicable prismatic block source, the filtered maps identify the outlines of the causative bodies, their susceptibility contrasts, and the approximate depths to the top of the edges. The technique has been applied to a variety of model and real data with very favorable results, and several of the more interesting model studies are described herein. Unfortunately, the proprietary nature of the real data cases precludes their publication at this time.

DERIVATION OF FILTER

Bhattacharyya (1964) has given the general equation for the total field due to a bottomless rectangular prism with a horizontal top surface. For polar regions (or for data reduced to the pole) the equation is greatly simplified and can be written as:

*Presented at the CSEG National Convention, Calgary, Alberta, April 19, 1974.

**Digitech Ltd., Calgary, Canada; formerly with Aero Service, Philadelphia, Pennsylvania.

***Aero Service, Philadelphia, Pennsylvania

†Manuscript received by the Editor, May 23, 1974.

$$\tau = k F \left| \tan^{-1} \frac{\alpha_1 \beta_1}{r_0 h} \right|_{\alpha_0 = \alpha_L}^{\alpha_U} \left| \beta_1 \right|_{\beta_0 = \beta_L} \dots (1)$$

where

τ = Total field due to the body

F = Inducing field of the earth

k = Susceptibility contrast

$\alpha_U, \alpha_L, \beta_U, \beta_L$ = coordinates of the body assumed parallel to the coordinate system.

$\alpha_1 = \alpha_0 - x$

$\beta_1 = \beta_0 - y$

x, y = Coordinates of the point of observation.

h = Depth to the top of the body.

$r_0^2 = \alpha_1^2 + \beta_1^2 + h^2$

Similarly, the second derivative of the total field in polar regions becomes:

$$\frac{\partial^2 \tau}{\partial z^2} = k F \left[\frac{\alpha_1 \beta_1 h}{r_0 (\alpha_1^2 \beta_1^2 + r_0^2 h^2)} \left\{ \frac{2(\alpha_1^2 + \beta_1^2) h^2}{\alpha_1^2 \beta_1^2 + r_0^2 h^2} - \frac{h^2}{r_0^2} \right\} \right]_{\alpha_0 = \alpha_L}^{\alpha_U} \left| \beta_1 \right|_{\beta_0 = \beta_L} \dots (2)$$

Equation (2) shows that for all but very narrow prismatic bodies, the second-derivative anomaly contains a maximum and a minimum for each horizontal edge of the body, the edge itself being closely marked by the zero contour (Vacquier, et al, 1951). A little algebraic manipulation of these equations makes it possible to use these highs and lows in the map to approximately determine the depth of the edge of the prism and the susceptibility contrast across the edge.

Depth to the Edge

Some elementary algebraic manipulation shows that the distance (d) between the plotted locations of maximum and minimum points is related to the depth (h) to the edge as follows:

$$d = C \cdot h \dots (3)$$

where C is a factor which ranges from 1.2 for very thin or very wide bodies to about 1.4 for bodies whose width is about twice the depth. If C is assumed equal to 1.3 universally, depth estimates within 10% can be expected when other conditions are met.

Susceptibility Contrast

If the edges of the body are all at least $4h$ in length, the following relationship can

be proved by some simple computing with equation (2):

$$\left(\frac{\partial^2 \tau}{\partial z^2} \right)_{\max} = 1.7 k F / h^2 \dots (4)$$

Thus, for any given depth (h), equation (4) can be used to compute a susceptibility factor. When the true second derivative operator (Mesko, 1966, Fuller, 1967) is multiplied by this factor and applied to the total field, the maxima in the second derivative map will correspond to the susceptibility contrast for bodies located at depth h , while the bodies themselves will be outlined fairly accurately by the zero contour of the second derivative (Vacquier, et al, 1951). In practice, the depths are estimated from the locations of the second derivative highs and lows in accordance with equation (3). If the depth so determined is different from h , a correction factor must be applied to increase or decrease the computed susceptibility, depending on whether this depth is greater or less, respectively, than that originally assumed. These correction factors are presented in Figure 1. In addition, a multiplying factor can be computed from equation (2) for correcting the susceptibilities when the width and/or length of the body is not at least four times the depth. A chart presenting the factors for various dimensions is shown in Figure 2.

Magnetic Data not in Polar Regions

Baranov (1957) used Poisson's theorem to derive the relationship between the observed total field in non-polar regions and the magnetic field and its derivatives at the pole. This relationship (see also Baranov and Naudy, 1964) makes it practical to apply the depth, susceptibility and outline determination methods described above to all magnetic data. Thus, a convolution of reduction to the pole and the true second derivative operators, followed by the scaling of amplitudes with a susceptibility factor as described above, provides an operator which can be used directly on the total field maps. The output of this operation provides depth estimates, susceptibility contrasts and the outlines of the causative bodies directly on a computed map. Inasmuch as these maps provide all relevant information concerning

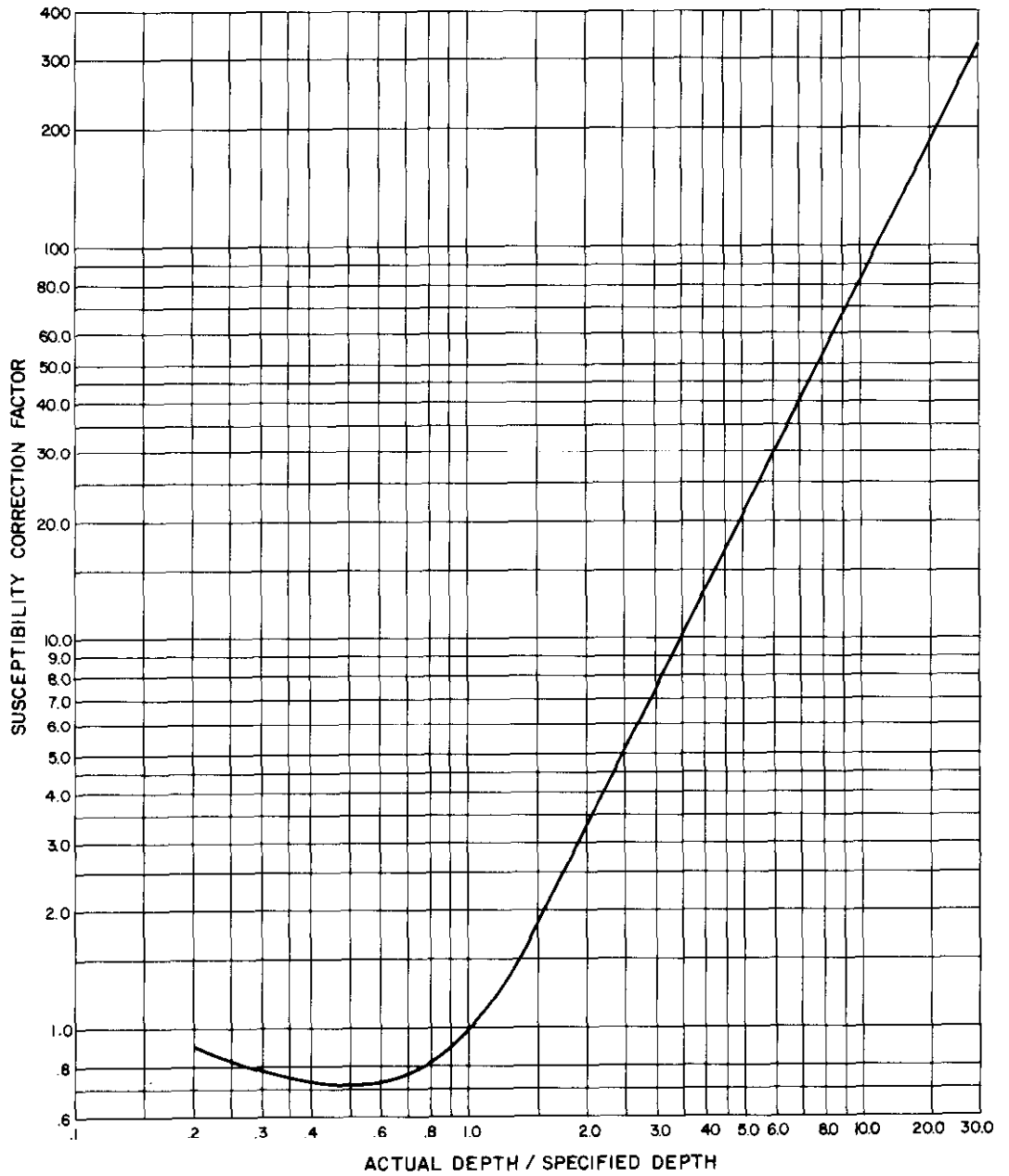


Fig. 1. Susceptibility correction factors for sources at depths different than specified.

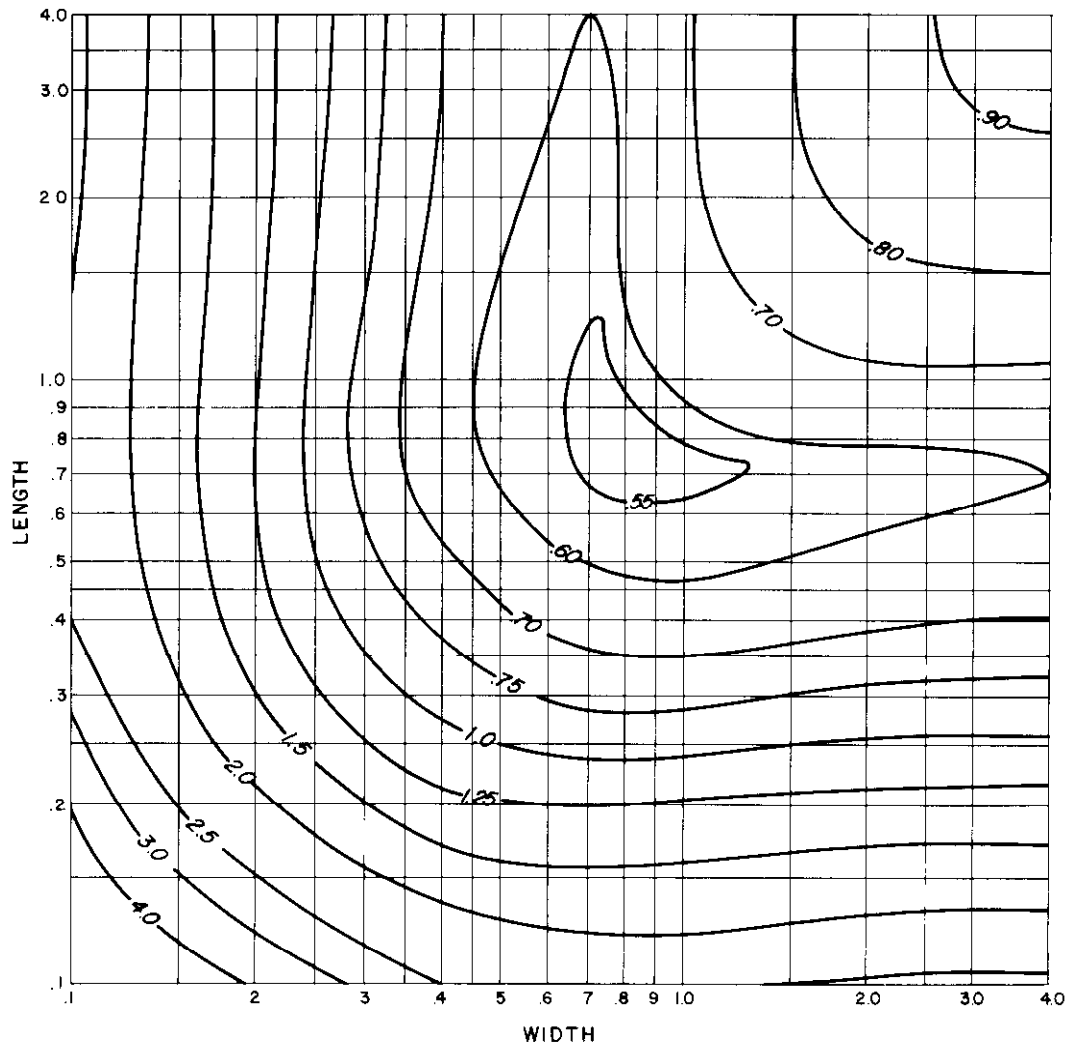


Fig. 2. Susceptibility correction factors for small prismatic bodies.

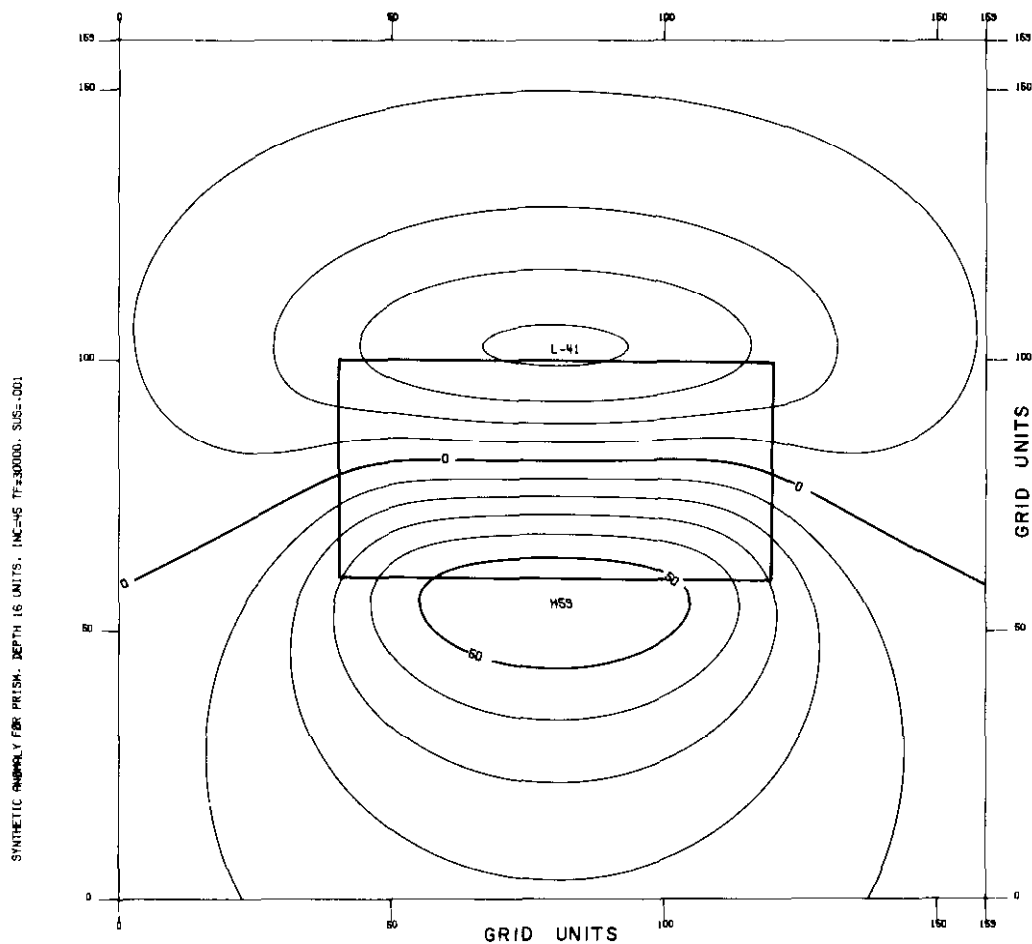


Fig. 3. Theoretical total field anomaly for a prismatic body at 45° N. inclination. Depth = 16 units; susceptibility contrast (k) = .001 c.g.s. units; intensity of earth's field (F) = 30,000 gammas.

the sources of the observed anomalies, they are termed SOURCE PARAMETER MAPS.

As an example of this procedure, let us examine a simple prismatic source at a magnetic inclination of 45° . The total field anomaly for this body is shown in Figure 3. The body is at a depth of 16 units of grid interval, and has an assigned susceptibility contrast of 0.001 c.g.s. units. Figure 4 presents the second derivative of the total field after reduction to the pole. The outline of the body is very closely approximated by the zero contour. One of the several indices which may be used to estimate depth is in-

dicated on the left side of the body, and one of the second derivative maxima used to estimate susceptibility contrast is similarly noted. In this particular example, the second derivative maxima have not yet been multiplied by a scaling factor. Both the depth calculated from the derivative anomaly (16 units), and the computed susceptibility contrast after scaling (0.0014 c.g.s. units), were found to be essentially coincident with the original body parameters.

In using these techniques in the case of real data, it should be recognized that the inadequacy of the grid (sampling) interval

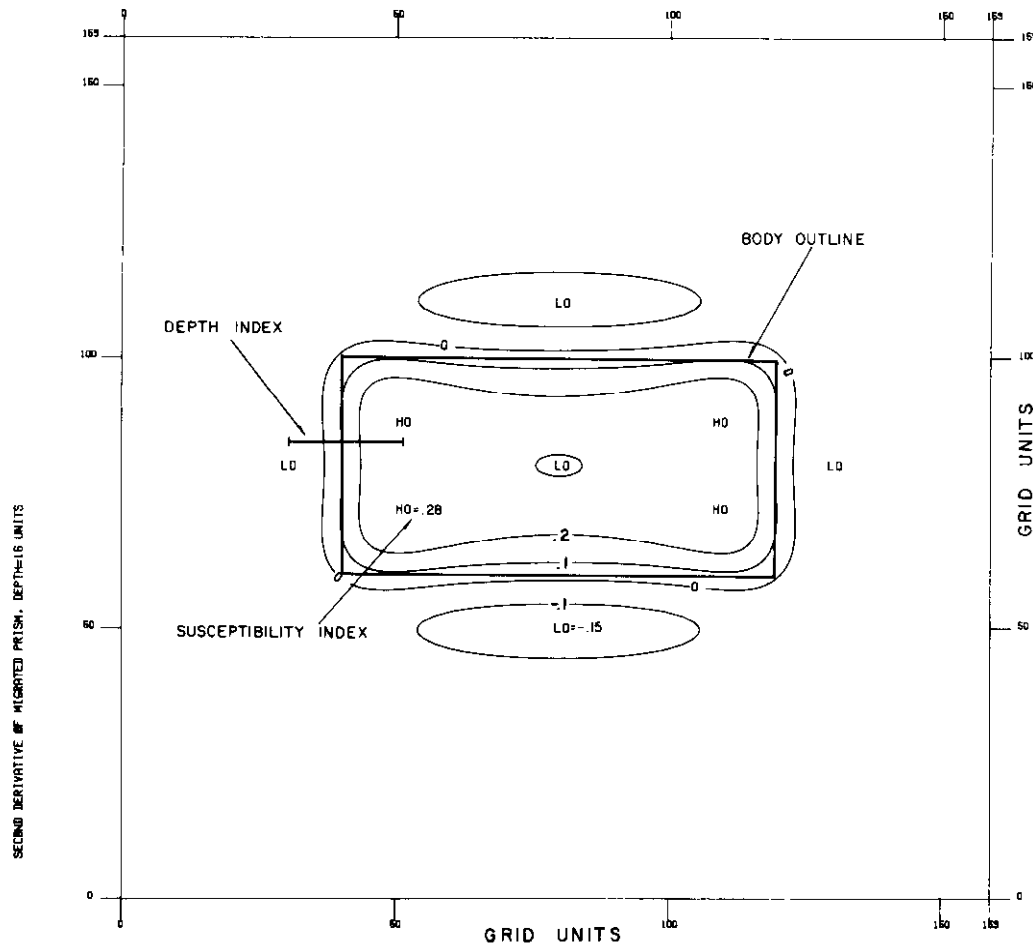


Fig. 4. Second vertical derivative of the total field anomaly shown in Figure 3 after migration to the pole, illustrating SOPAM interpretation parameters.

and/or the insufficient size of the SOPAM operator sometimes leave the reduction to the pole incomplete. In such cases, the value of constant C in equation (3) may be as high as 1.5 when dealing with an east-west edge. The edges extending north-south are not affected by inadequate reduction to the pole and, therefore, are preferred for depth estimation as a general practice.

MODEL EXPERIMENTS

In addition to the foregoing example, a variety of more complex models were generated to study the source parameter maps

under controlled conditions. Three of these models will be briefly described.

CASE 1: MODEL WITH TEN BODIES AT VARIOUS ORIENTATIONS

To simulate an area with near-surface sources, a model with ten bodies with various orientation and sizes was computed (Figure 5). The source parameter map for this configuration is shown in Figure 6. The outlines of the bodies are marked very accurately but the susceptibility contrasts are about 15-30% less than the actual values. This is consistent with the results of other

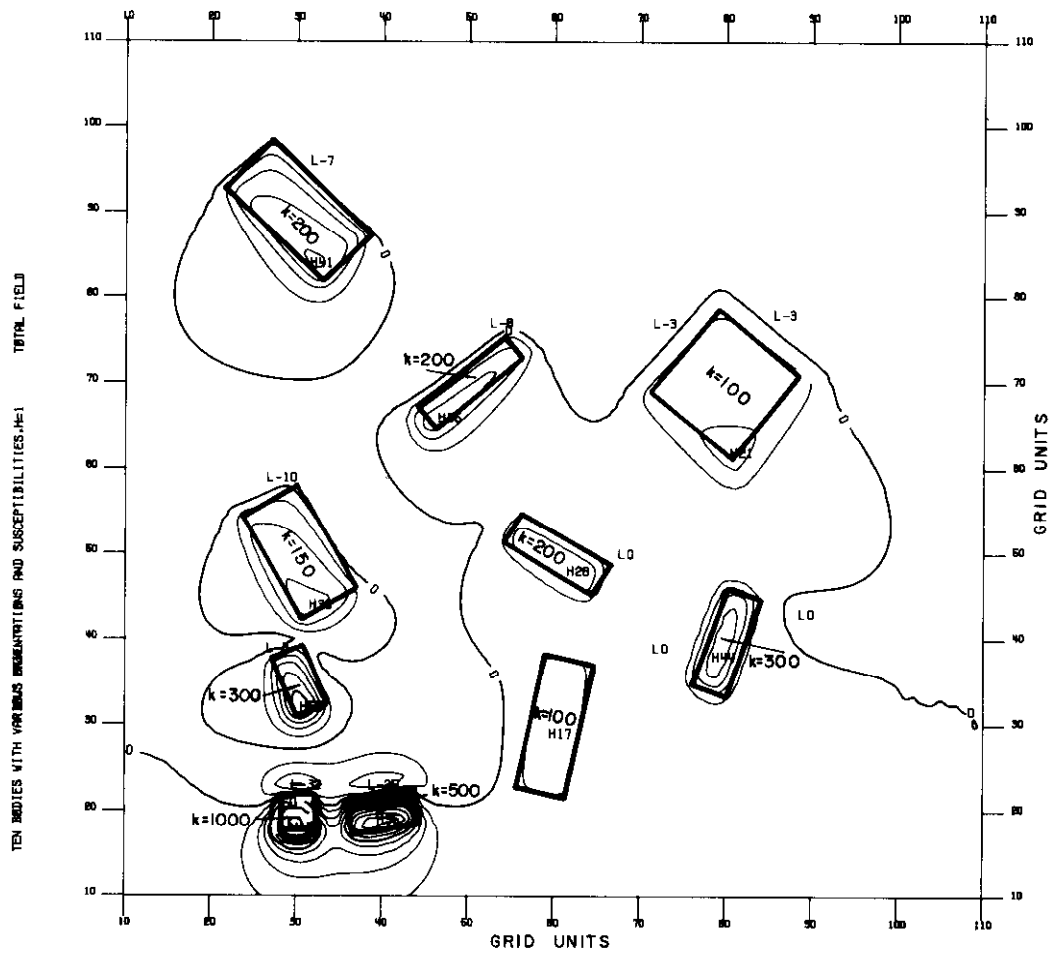


Fig. 5. Theoretical total field response over ten prismatic bodies. The depth of all bodies is one grid unit. Assigned susceptibility contrasts (k) are in c.g.s. units $\times 10^{-6}$. The total intensity of the earth's magnetic field (F) = 30,000 gammas; inclination (I) = $60^\circ N$.

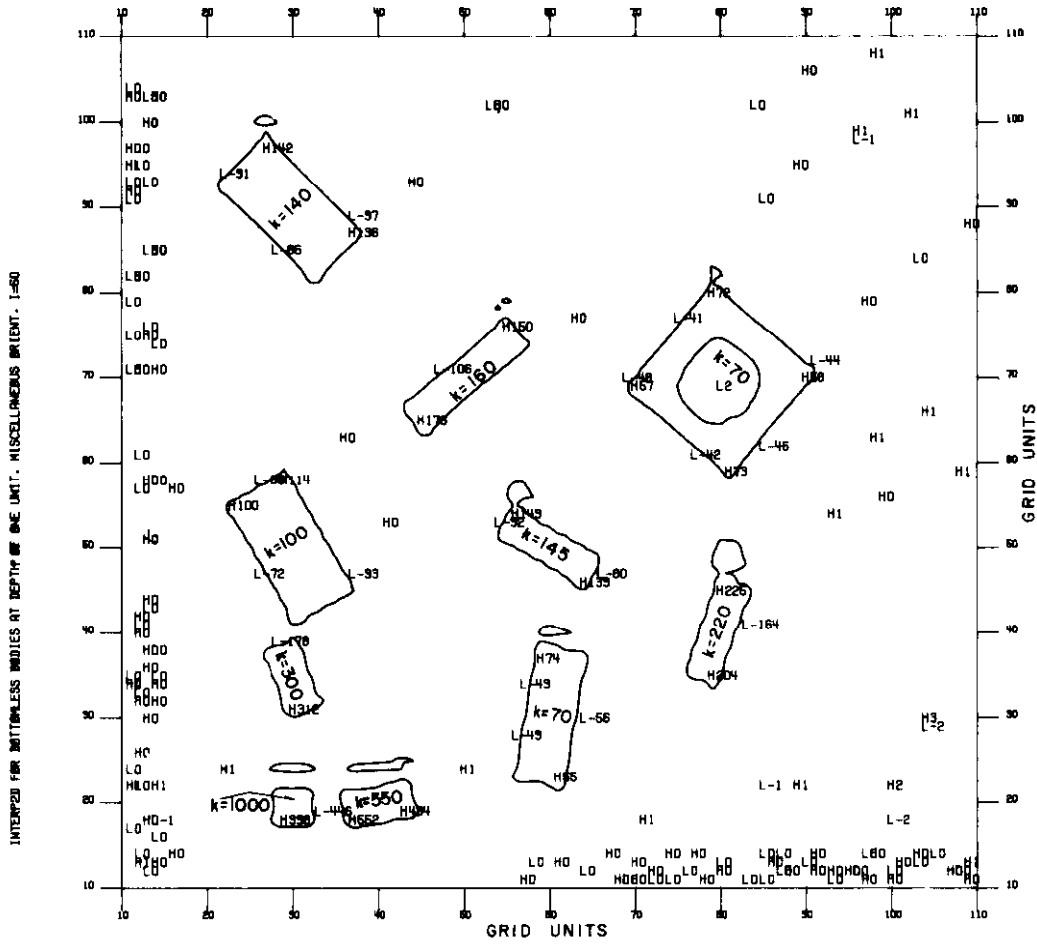


Fig. 6. Source parameter map of the model data shown in Figure 5, computed for a depth of one grid unit. Average interpreted susceptibility contrasts (k) are in c.g.s. units $\times 10^{-6}$.

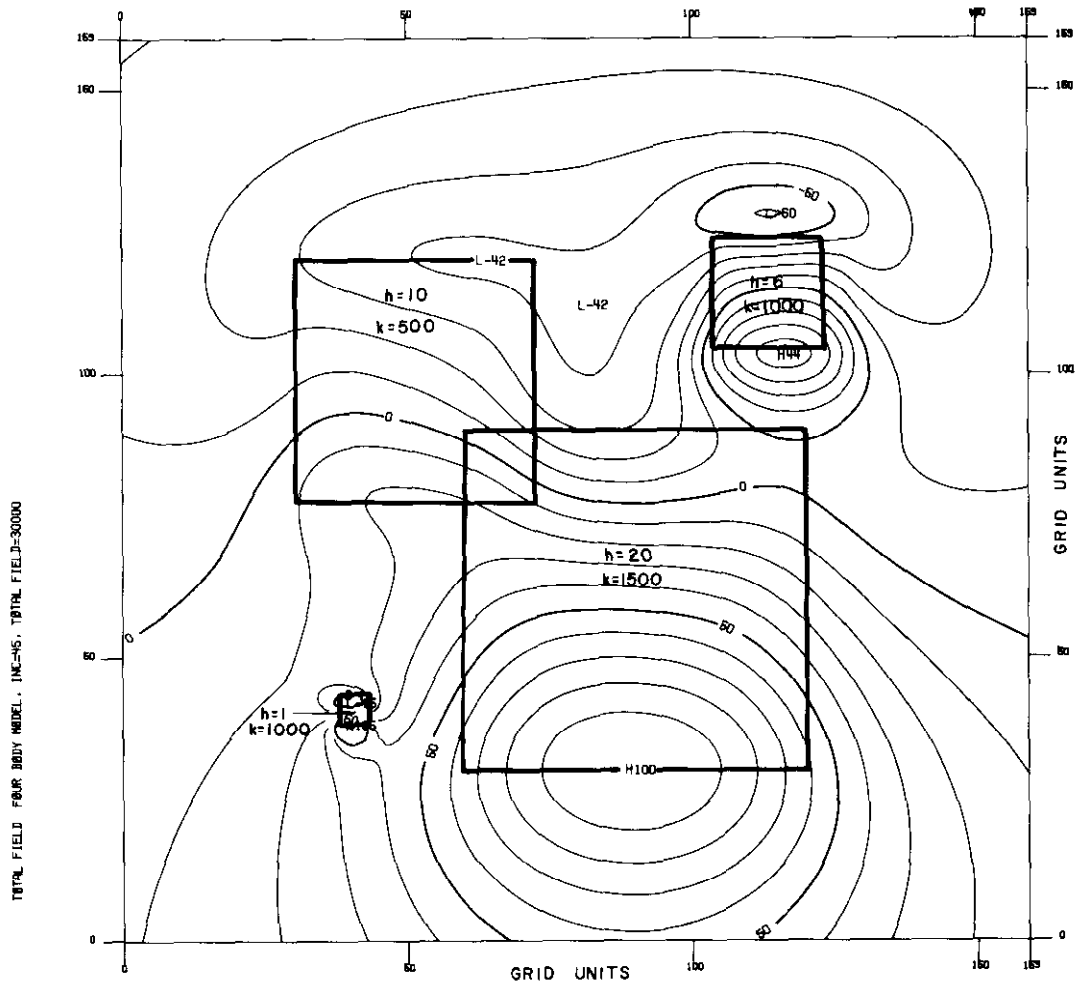


Fig. 7. Theoretical total field response over four prismatic bodies at various depths. Depths (h) are in grid units; susceptibility contrasts (k) are in c.g.s. units $\times 10^{-6}$. The total intensity of the earth's magnetic field (F) = 30,000 gammas; inclination (I) = $45^\circ N$.

model experiments, however, and reflects inadequate sampling of the data for such shallow sources.

CASE 2: MODEL WITH FOUR BODIES AT VARIOUS DEPTHS

Figure 7 shows the total field due to four prismatic bodies, the depths to the tops being 1, 6, 10, and 20 units of grid interval. The relevant parameters of the sources are given in the figure.

The source parameter map for the model is given in Figure 8. This operator was

computed for an average source depth of 6 units. The shallow body, at 1 unit of depth, is not outlined as well as the deeper bodies because the sampling interval of the operator selected for this particular example was too large for the small anomaly describing this source. The deepest body, at 20 units of depth, is estimated to have greater susceptibility (after correction) than it actually does (3500 vs 1500 $\times 10^{-6}$ c.g.s. units). In this case, the operator length is not adequate for such deep bodies, and the computed susceptibility contrast is in error. The depths to all three of the deep bodies, how-

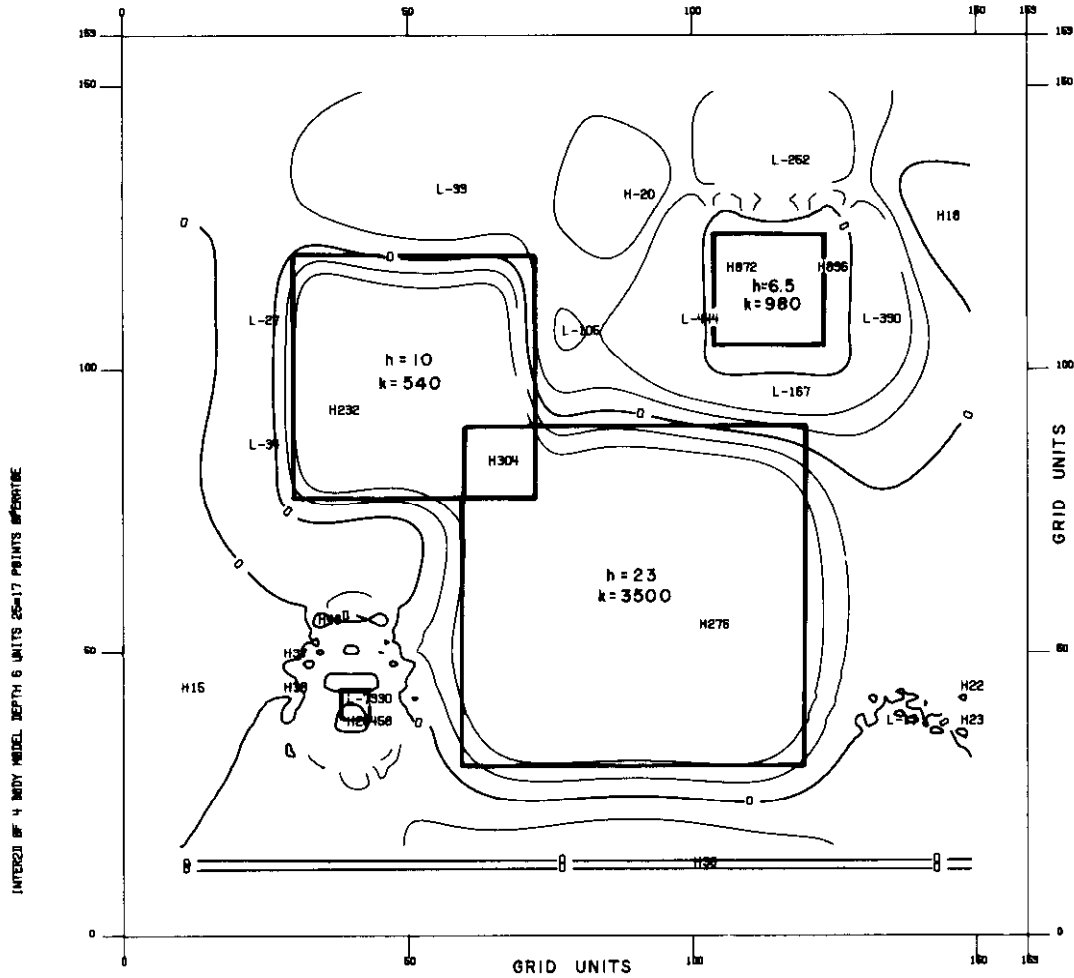


Fig. 8. Source parameter map of the model data shown in Figure 7, computed for a depth of six grid units. Interperated depths (h) are in grid units and susceptibility contrasts (k) are in c.g.s. units $\times 10^{-6}$.

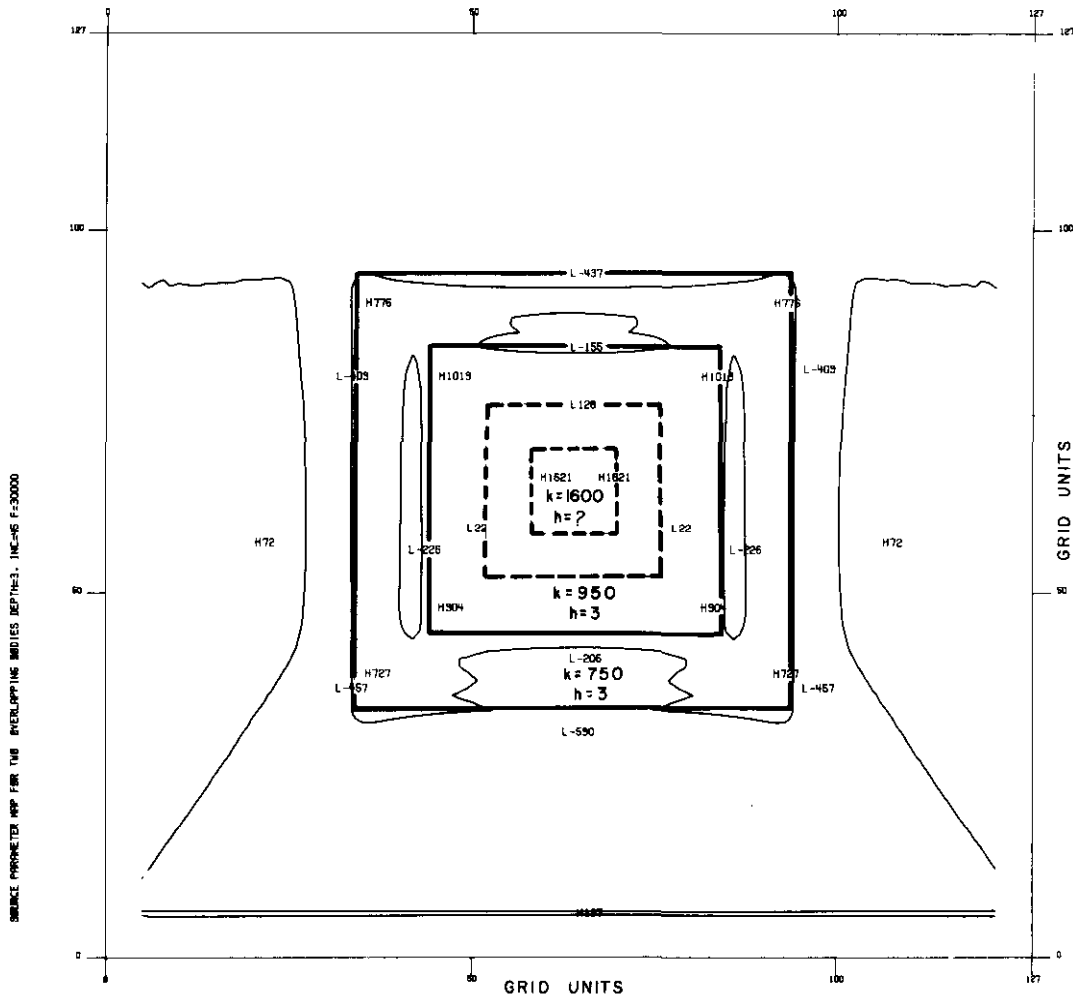


Fig. 10. Source parameter map of the model data shown in Figure 9, computed for a depth of three grid units. Interpreted depths (h) are in grid units; susceptibility contrasts (k) are in c.g.s. units $\times 10^{-6}$.

the source parameter map averages their susceptibility and does not provide depth or boundary parameters.

their assistance in preparing the manuscript and illustrations, respectively.

CONCLUSIONS

As demonstrated by the preceding examples, the SOPAM technique provides, directly and rapidly on a single map, a considerable amount of useful information concerning the sources of magnetic anomalies which is applicable to both petroleum and mining survey work. Its basic use is as an interpretation aid to provide initial information which can then be further refined by more precise quantitative techniques, such as profile methods. However, since it is a complete method in itself, it could certainly have application as a rapid means of obtaining a preliminary evaluation of an area, as well.

ACKNOWLEDGEMENTS

The authors wish to thank Aero Service for permission to present this paper. They would also like to thank Mrs. Jane Rigau, and Messrs. L. Goldberg and C. Morgan for

REFERENCES

- Baranov, V., 1957. A new method of interpretation of aeromagnetic maps, pseudo-gravimetric anomalies. *Geophysics*, 22, 359-383.
- Baranov, V., and Naudy, H., 1964. Numeric calculation of the formula of reduction to the pole. *Geophysics*, 29, 67-79.
- Bhattacharyya, B. K., 1964. Magnetic anomalies due to prism-shaped bodies with arbitrary polarisation. *Geophysics*, 29, 517-531.
- Fuller, B. D., 1967. Two dimensional frequency analysis and design of grid operators. *Mining Geophysics*, Vol. 2, Soc. of Explor. Geoph., 658-708.
- Mesko, C. A., 1966. Two dimensional filtering and the second derivative method. *Geophysics*, 31, 606-615.
- Vacquier, V., Steenland, N. C., Henderson, R. G., and Zietz, I., 1951. Interpretation of aeromagnetic maps. *Geol. Soc. Amer. Mem.* 47.